Comparison of a DSB-120 DNA Interstrand Cross-Linked Adduct with the Corresponding Bis-tomaymycin Adduct: An Example of a Successful Template-Directed Approach to Drug Design Based upon the Monoalkylating Compound Tomaymycin

John A. Mountzouris,† Jeh-Jeng Wang,† David Thurston,‡ and Laurence H. Hurley*,†

Drug Dynamics Institute, College of Pharmacy, The University of Texas at Austin, Austin, Texas 78712-1074, and School of Pharmacy and Biomedical Sciences, University of Portsmouth, King Henry I Street, Portsmouth, Hants PO1 2DZ, United Kingdom

Received May 9, 1994®

The interstrand cross-linked DSB-120-d(CICG*ATCICG)$_2$ DNA adduct (* indicates covalently modified guanine) was examined by two-dimensional NMR and compared to the bis-tomaymycin adduct on the same oligomer. Tomaymycin and DSB-120 form self-complementary adducts with the d(CICGATCICG)$_2$ duplex sequence in which the covalent linkage sites occur between C11 of either drug and the exocyclic 2-amino group of the single reactive guanine on each strand of d(CICGATCICG)$_2$. In the case of DSB-120, this is evidence for the formation of a guanine–guanine DNA interstrand cross-link. Both drugs show formation of an *S* stereochemistry at the covalent linkage site with an associated 3′ orientation. While the majority of DNA in these adducts appears to be B-form, DSB-120 interstrand cross-linking induces atypical properties in the 8I nucleotide, indicated by broadening of the 8IH2 proton resonance, non-C2′ endo sugar geometry, and unusually weak internucleotide NOE connectivity to the 7C nucleotide. Tomaymycin does not produce this regional dislocation. For tomaymycin, while there are strong NOE connectivities from protons on the five-membered ring to the 8IH2 proton on the floor of the minor groove, the equivalent internucleotide connectivities in DSB-120 are weaker. This indicates that the tomaymycin tail is close to the floor of the minor groove, while the five-membered ring of DSB-120 is more shallowly immersed, perhaps due to strain from cross-linking with a very short linker unit. Last, the conformational stresses induced on the duplex by DSB-120 appear to make the region of covalent attachment more accessible to solvent than is the case for tomaymycin. The 4GN2H$_b$ resonance appears in 100% D_2O on the tomaymycin adduct but is only observed in 90% H_2O/10% D_2O for the DSB-120 adduct. On the basis of these results, the strategies for template-directed DNA cross-linker design are assessed.

Introduction

DSB-120 (1,1′-(propane-1,3-diyldioxy)bis[(11a*S*)-7-methoxy-1,2,3,11a-tetrahydro-5*H*-pyrrolo[1,2-c][1,4]-benzodiazepin-5-one]) is a synthetic antitumor agent incorporating a pair of DNA alkylating units based on the monofunctional DNA-reactive moiety of the pyrrolo-[1,4]benzodiazepines (P[1,4]Bs) (Figure 1), which have been linked through O8 by a trimethylene bridge.[1] The P[1,4]Bs, which include tomaymycin, have been proposed to covalently bond to N2 of guanine to form a neutral minor groove adduct[2] (Figure 2), although recent evidence points to a positively charged species.[3] The cytotoxic and antitumor effects of these compounds are believed to arise from modification of DNA, which leads to inhibition of nucleic acid synthesis[4] and production of excision-dependent single- and double-strand breaks in cellular DNA.[5] The sequence selectivity of tomaymycin and anthramycin covalent bonding to DNA has been ranked by chemical and enzymatic footprinting of DNA restriction fragments by methidiumpropyl EDTA·Fe(II)[6] and exonuclease III[7] to be 5′PuGPu> 5′PuGPy~5′PyGPu>5′PyGPy, although a recent study

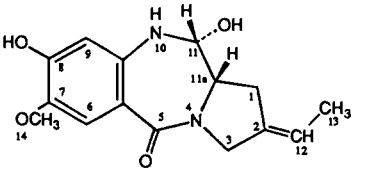

1

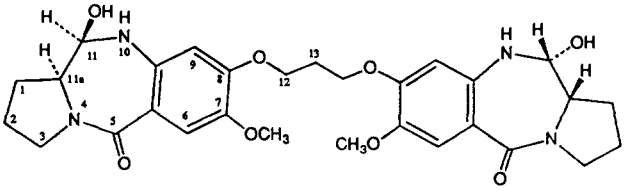

2

Figure 1. Structures of P[1,4]Bs tomaymycin (1) and DSB-120 (**2**).

using the UVrABC endonuclease indicated that there are differences between tomaymycin and anthramycin and that tomaymycin shows a preference for cytosine to the 3′ side of the covalently modified guanine.[8] For anthramycin, clinical acceptance was precluded by dose-limiting cardiotoxicity.[9] Synthetic monoalkylating analogs devoid of cardiotoxicity manifest relatively poor *in vitro* and *in vivo* potency.[7]

* Address correspondence to this author. Tel: (512) 471-4841. Fax: (512) 471-2746.
† The University of Texas at Austin.
‡ University of Portsmouth.
® Abstract published in *Advance ACS Abstracts*, August 1, 1994.

0022-2623/94/1837-3132$04.50/0

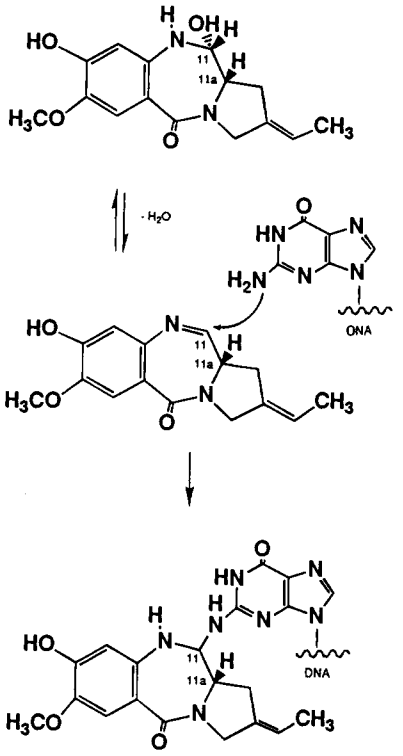

Figure 2. Proposed reaction of tomaymycin with guanine in DNA.[2c]

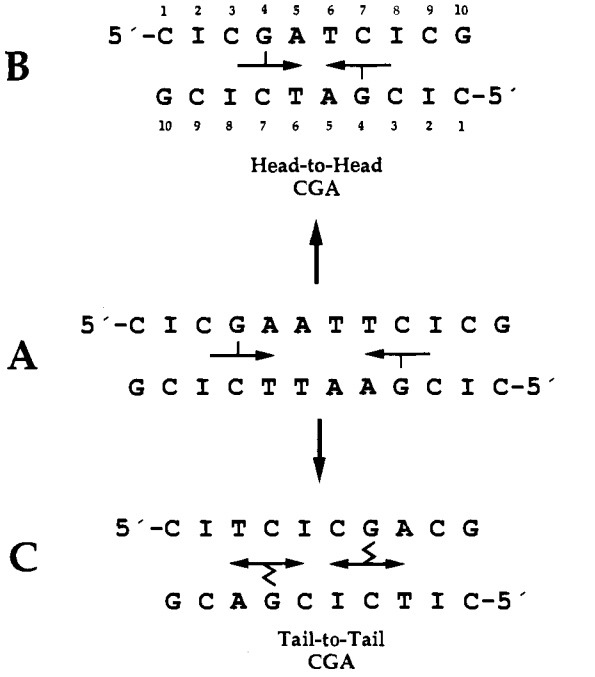

Figure 3. DNA sequences examined for template-directed bis-tomaymycin alkylation: sequence A,[16a] sequence B,[16b] and sequence C.[16b]

The design inspiring the synthesis of DSB-120 rests on several principles. A number of antitumor agents, such as mitomycin C, *cis*-platinum, and nitrogen mustards, have the capability to form intra- or interstrand cross-links on DNA.[10] The interstrand cross-linking of DNA by mitomycin C and the nitrogen mustards is proposed to be responsible for the high potency of these compounds.[11] The concept of synthesizing tethered monoalkylating DNA-reactive units to form an interstrand cross-linker has been previously enacted.[12] For example, dimeric analogs incorporating the DNA-alkylating cyclopropylindole (CPI) unit from the natural product (+)-CC-1065 have been made.[12a] One of these dimeric analogs, Bizelesin (The Upjohn Co.), which is in phase I clinical trials, is more potent and efficacious than its parent monoalkylating compound.[12a] Work in our laboratory on Bizelesin has highlighted other reasons for the design of DNA cross-linkers. As a result of cross-linking, Bizelesin induces an unexpected structural transition to Hoogsteen base pairing in the internal region of cross-linked oligonucleotides,[13] and the capability to bisalkylate DNA alters the sequence selectivity relative to (+)-CC-1065.[14] Besides the possible therapeutic potential, creating novel distortion in DNA structure and targeting new sequences for alkylation are attractive reasons to continue designing DNA cross-linking agents.

The P[1,4]B dimer DSB-120 exhibits efficient irreversible interstrand cross-linking, as shown by gel electrophoresis.[1,15] A previous cross-linking analog in which the P[1,4]B nucleus was linked through C7 (Figure 1) was shown to be highly reversible by a simple pH change.[12b] Sequence specificity studies suggest that DSB-120 prefers a central AT base-pair motif embedded between the covalently modified cross-linked guanines.[1]

In a template-directed approach to the design of DNA–DNA cross-linkers, we have characterized a series of self-complementary bis-tomaymycin–DNA adducts using the combined approach of two-dimensional NMR and molecular modeling (Figure 3).[16] Our discovery of a sequence-dependent minor groove orientation of tomaymycin and a sequence-dependent stereochemistry at the covalent linkage site had important implications for the design of an interstrand DNA cross-linker. Sequence A is a derivation of the well-characterized Dickerson dodecamer d(CGCGAATTCGCG)$_2$, in which two guanines have been replaced by inosines to create a self-complementary duplex with only one unique bonding site for the drug at 4G on each strand. Tomaymycin forms a nondistortive *head-to-head* self-complementary bis-adduct with sequence A, with both drugs displaying *S* stereochemistry at the covalent linkage site and the aromatic ring oriented to the 3′ side of the covalently modified guanine.[16a] A 3′*S* self-complementary bis-adduct is also exhibited in the truncated decamer sequence B, which is formed by the excision of the two central AT base pairs from sequence A.[16b] In this sequence, the O8 phenol positions are separated by approximately 6.8 Å, appropriate for joining by a short aliphatic bridge. In contrast, efforts to use a template-directed approach to design a defined *tail-to-tail* adduct using sequence C, which has the same triplet bonding sequence as sequence B, resulted in a complex adduct mixture with more than one species of tomaymycin bound to DNA.[16b] From the template-directed approach to the design of a sequence-directed DNA bis-alkylation, a P[1,4]B–DNA interstrand cross-linker in which two tomaymycin units were linked head to head by a flexible methylene bridge was proposed and subjected to molecular modeling.[16b]

The two-dimensional NMR data for the DSB-120 and bis-tomaymycin d(CICGATCICG)$_2$ 10-mer adducts (sequence B) were examined to determine the predictive value of the template-directed approach.

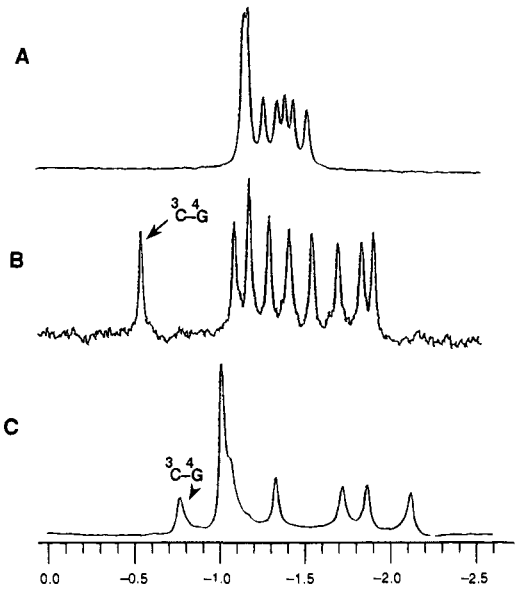

Figure 4. One-dimensional proton-decoupled 202.44-MHz phosphorus NMR spectra in 0.5 mL of D_2O-buffered solution, pH 6.8, 100 mM sodium chloride, and 10 mM sodium phosphate at 23 °C for the (A) d(CICGATCICG)$_2$ duplex, (B) bis-tomaymycin adduct, and (C) DSB-120 adduct.

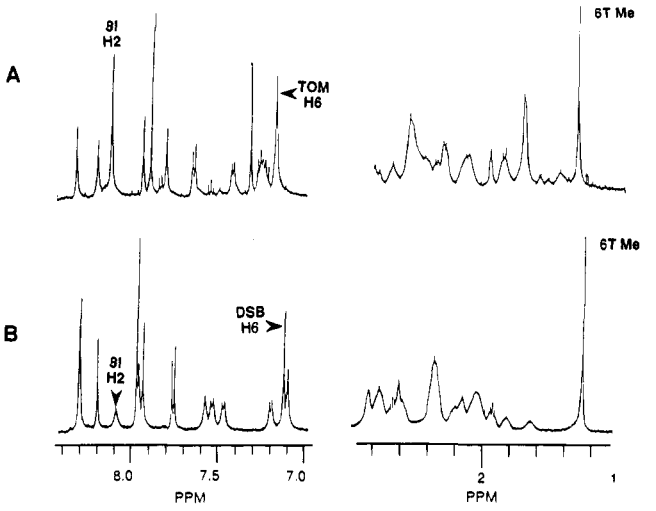

Figure 5. Expansions of one-dimensional nonexchangeable NMR spectra in 0.5 mL of D_2O-buffered solution, pH 6.8, 100 mM sodium chloride, and 10 mM sodium phosphate at 23 °C showing, left to right, the respective aromatic and methyl regions for the (A) bis-tomaymycin d(CICGATCICG)$_2$ adduct and (B) DSB-120 d(CICGATCICG)$_2$ adduct.

Results

Prior to making a comparison of the DSB-120 and bis-tomaymycin 10-mer duplex adduct structures, it was necessary to determine the complexity of the cross-linked species formed, identify the covalent linkage sites between DSB-120 and DNA, and determine the stereochemistry and orientation of the DSB-120 species on DNA.

Symmetry of the DSB-120 10-mer Duplex Adduct. A. Phosphorus Spectra. The proton-decoupled phosphorus spectra of the 10-mer duplex, the bis-tomaymycin adduct, and the DSB-120 adduct in D_2O buffer are plotted in panels A, B, and C of Figure 4, respectively. Nine phosporus resonances are detected for the bis-tomaymycin adduct (Figure 4B) and the DSB-120 adduct (Figure 4C), using two-dimensional heteronuclear phosphorus-detected $^{31}P-^{1}H$ phase-sensitive relayed correlated spectroscopy (COSY) coupling connectivities to H3′ protons in the 5′ direction and H4′ protons in the 3′ direction (data not shown). This is the same number that is necessarily present in the overlapped spectra of the duplex (Figure 4A) and establishes that the 2-fold symmetry of the self-complementary duplex is maintained in both the bis-tomaymycin and DSB-120 adducts. There is greater dispersion of the phosphorus resonances in the tomaymycin– and DSB-120–DNA adducts. The downfield-shifted phosphorus (3C–4G step) to the 5′ side of the covalently modified guanine has been previously used as a probe of modest distortion in the deoxyribose phosphate backbone induced by bonding of tomaymycin to short oligomers.[3,16a] A similar perturbation in chemical shift is also evident for the DSB-120 adduct.

B. Nonexchangeable Proton Assignments. The one-dimensional ^{1}H-NMR nonexchangeable aromatic and methyl resonances for the bis-tomaymycin and DSB-120 adducts are plotted in Figure 5A, B, respectively. The majority of the signals are well resolved and have been assigned by two-dimensional NMR spectra employing through-bond COSY and through-space nuclear overhauser effect spectroscopy (NOESY) connectivities. The chemical shift assignments for the nucleotide and drug protons in the duplex and the two adducts are listed in Table 1. It is worthwhile to note that 8IH2 is unusually broad in the DSB-120 10-mer adduct but not in the bis-tomaymycin adduct (Figure 5). This suggests that cross-linking induces conformational exchange in a restricted area on the strand opposite the covalently modified guanine. Other unusual features of the 8I nucleotide unique to DSB-120–DNA interstrand cross-linking are noted later.

The same number of DNA proton resonances exists in both the duplex and the tomaymycin and DSB-120 adducts. The single 6T methyl and 8IH2 resonances are designated as examples in Figure 5. A single set of resonances is assigned to both tomaymycin molecules in the bis-adduct, confirming the self-complementarity of the adduct (Table 1C). Likewise, a single set of resonances describing both halves of DSB-120 confirms symmetry about the methylene bridge in this DNA adduct (Table 1C). The single H6 aromatic protons of tomaymycin and DSB-120 in their respective 10-mer adducts are shown as examples (Figure 5).

Identification of the Covalent Linkage Site. Chemical shift assignments for exchangeable DNA and drug protons are listed in Table 1. Significantly, the double-quantum-filtered correlated spectroscopy (DQF-COSY) experiments exhibit scalar coupling between the slowly exchanging 4GN2H$_b$ and the C11 proton in both the DSB-120 (90% H_2O/10% D_2O buffer, pH 6.8) and tomaymycin (D_2O buffer, pH 6.8) DNA adducts (supplementary information and unpublished results). These scalar couplings have a precedent in the COSY spectra of the covalent DNA adducts of other P[1,4]Bs, including tomaymycin,[16a] and conclusively establish that both drugs achieve covalent attachment via C11 to the 4G exocyclic 2-amino nitrogens of the duplex. In the case of DSB-120, this is unequivocal evidence for the formation of a symmetrical DNA–DNA interstrand cross-link.

Importantly, while the normally exchangeable 4GN2H$_b$ proton is restricted enough in motion and/or solvent exchange to be visible in the one-dimensional NMR

Table 1

A. Base Proton NMR Chemical Shifts (ppm) for d(ClCGATCICG)$_2$ (10-mer), Bis-tomaymycin d(CICGATCICG)$_2$ (T-mer), and DSB-120 d(CICGATCICG)$_2$ (DSB-120-mer) Adducts[a]

assignment	10-mer	T-mer	DSB-120-mer	assignment	10-mer	T-mer	DSB-120-mer
			Aromatic Protons				
1CH6	7.60	7.60	7.72	1CH5	5.88	5.86	5.93
2IH8	8.25	8.25	8.26	2IH2	7.84	7.83	7.93
3CH6	7.36	7.36	7.50	3CH5	5.31	5.30	5.52
4GH8	7.73	7.73	7.92				
5AH8	8.06	8.06	8.26	5AH2	7.72	8.05	8.16
6TH6	7.11	7.11	7.07	6TMe	1.30	1.34	1.27
7CH6	7.47	7.19	7.17	7CH5	5.59	5.35	5.31
8IH8	8.13	8.13	8.05	8IH2	7.76	7.26	7.54
9CH6	7.21	7.21	7.44	9CH5	5.36	5.29	5.52
10GH8	7.88	7.88	7.89				
			Imino Protons and 4GN2H$_b$ (15 °C)				
1C-10G		13.45	12.90	4G-7C	13.41	12.95	12.80
2I-9C		15.35	15.10	5A-6T	12.42	13.70	13.50
3C-8I	15.20	15.35	15.10	4GN2H$_b$		8.94	9.10

B. Deoxyribofuranose Proton NMR Chemical Shifts (ppm) for d(CICGATCICG)$_2$ (10-mer), Bis-tomaymycin d(CICGATCICG)$_2$ (T-mer), and DSB-120 d(CICGATCICG)$_2$ (DSB-120-mer) Adducts

	H1′			H2′			H2″			H3′			H4′		
assign-ment	10-mer	T-mer	DSB-120-mer	10-mer	T-mer	DSB-120-mer	10-mer	T-mer	DSB-120-mer	10-mer	T-mer	DSB-120-mer	10-mer	T-mer	DSB-120-mer
1C	5.61	5.55	5.74	1.94	1.93	1.92	2.36	2.32	2.38	4.68	4.66	4.62	4.02	4.02	3.98
2I	6.21	6.18	6.21	2.75	2.69	2.81	2.90	2.85	2.81	5.01	4.97	4.94	4.441	4.37	4.37
3C	5.76	5.40	5.43	1.75	2.15	2.05	2.29	2.39	2.30	4.82	4.81	4.82	4.22	4.16	4.10
4G	5.56	6.08	6.16	2.73	2.54	2.71	2.76	2.89	3.05	5.00	5.00	5.06	4.36	4.37	4.12
5A	6.21	6.15	6.44	2.60	2.52	2.60	2.91	2.56	2.75	4.96	4.93	4.98	4.45	4.23	4.15
6T	5.88	5.67	5.78	2.00	1.88	2.03	2.45	2.45	2.19	4.83	4.58	4.62	4.26	1.98	2.61
7C	5.58	5.76	5.48	2.06	1.75	1.65	2.38	2.18	2.15	4.84	4.79	4.72	4.22	4.18	4.07
8I	6.17	5.78	5.86	2.70	2.56	2.73	2.88	2.56	2.56	5.02	4.85	4.89	4.41	3.84	3.79
9C	5.82	5.80	5.83	1.65	1.49	1.82	2.21	2.21	2.34	4.80	4.73	4.72	4.22	4.03	4.08
10G	6.11	6.09	6.12	2.61	2.56	2.64	2.37	2.32	2.34	4.66	4.66	4.65	4.15	4.15	4.15

C. Tomaymycin and DSB-120 Proton NMR Chemical Shifts (ppm) in Respective d(CICGATCICG)$_2$ Adducts

drug	H1A	H1B	H2A[b]	H2B[b]	H3A	H3B	H6	7OCH3	8OH[c]	H9	H11	H11A	H12[c]	H12[b]	H13[c]	H13[b]
tomaymycin	2.80	3.00			3.13	3.87	7.11	3.87	9.34	6.51	5.56	4.03	5.86		1.74	
DSB-120	2.05	2.30	2.03	2.14	3.58	3.83	7.09	3.87		6.59	5.75	3.83		4.28		2.33

[a] Chemical shifts underlined are >±0.25 ppm shifted from free duplex chemical shifts. [b] DSB-120. [c] Tomaymycin.

spectra in D_2O buffer for the tomaymycin 10-mer adduct, it is *not visible* for the DSB-120 10-mer adduct in the one-dimensional spectrum in D_2O buffer (supplemental information) or in the COSY experiment in D_2O buffer (not shown). This suggests that the region containing this proton has greater access to water for exchange in the case of the interstrand cross-linked adduct. This possibility is also supported by the conformational distortion that is unique to the DSB-120–DNA adduct, which is detected by the two-dimensional NMR results discussed later.

Stereochemistry and Orientation. *A priori*, either an *S* or *R* stereochemistry at the covalent linkage site C11 of the antibiotic is conceivable in P[1,4]B–DNA adducts.[2c,d] In previous studies, a combined molecular modeling, fluorescence, and two-dimensional NMR approach showed that, for the tomaymycin d(ATGCAT)$_2$ adduct, 11*R* and 11*S* stereoisomers exist in approximately equal proportions.[2c] In contrast, for the bis-tomaymycin decamer adduct (sequence A, Figure 3), only the *S* stereoisomer exists,[16a] and in the case of anthramycin–DNA adducts, single stereoisomers exist.[17] The proton attached to the C11 chiral carbon located at the covalent linkage site is useful as a diagnostic probe of the stereochemistry at this position. In the adduct with *S* stereochemistry at this site, H11 would be directed toward the 3′ side of the covalently modified guanine, while for *R* stereochemistry, this

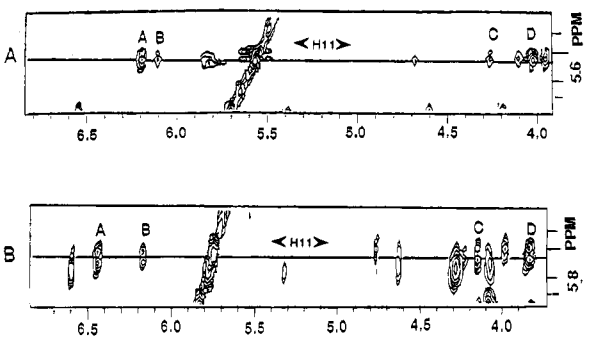

Figure 6. Expanded contour plot of the two-dimensional phase-sensitive NOESY spectrum (250-ms mixing time) of the (A) bis-tomaymycin d(CICGATCICG)$_2$ and (B) DSB-120 d(CICGATCICG)$_2$ duplex adducts in D_2O-buffered solution, pH 6.8, 100 mM sodium chloride, and 10 mM sodium phosphate at 23 °C, demonstrating through-space connectivities between P[1,4]B H11 and DNA protons. (A) Cross-peaks A–D are labeled as follows: A, tomaymycin(H11)–5A(H1′); B, tomaymycin(H11)–4G(H1′); C, tomaymycin(H11)–5A(H4′); D, tomaymycin(H11)–(H11a). (B) Cross-peaks A–D are labeled as follows: A, DSB-120(H11)–5A(H1′); B, DSB-120(H11)–4G(H1′); C, DSB-120-(H11)–5A(H4′); D, DSB-120(H11)–(H11a).

proton would point toward the 5′ side. There is a strong NOE between H11 and 5AH1′ for both the bis-tomaymycin and DSB-120 10-mer adducts (cross-peak A in Figure 6A, B, respectively) and to 5AH2 (data not shown). NOESY cross-peaks of H11 to base pairs to the

Table 2. Relative Strength of the Intermolecular Tomaymycin and DSB-120 NOEs to DNA for Each of the d(CICGATCICG)$_2$ Adducts[a]

DNA protons	drug protons														
	H1a	H1b	H2a[b]	H2b[b]	H3a	H3b	H6	H9	H11	H11a	H12a,b[b]	H13a,b[b]	7OCH$_3$[b]	H12[c]	H13[c]
3CH4′															
4GH1′									W/M		M				
5AH2								S/S			S	M			
5AH1′								W/W	S/S						
5AH2″								A/M							
5AH4′	A/W	A/W	W	W	A/M	M/S			W/M						
6TH1′								M/M			S				
6TH4′													W		
7CH1′								M/W			M				
7CH4′												S			
8IH2	M/W	M/W													M
8IH1′	M/W	M/W													M
8IH3′							A/W						W		
8IH4′					M/M	A/W	M/M								
9CH1′															W
9CH4′	A/W	A/W	W	W	A/M	A/M								W	S

[a] S = strong, M = medium, and W = weak (relative to the cytosine H5 to H6 cross-peak intensity). A = absent cross-peak. For protons in common, intermolecular tomaymycin cross-peak intensities are listed first followed by intermolecular DSB-120 cross-peak intensities. [b] Protons unique to DSB-120. [c] Protons unique to tomaymycin.

5′ side of 4G are absent. These observations provide strong evidence for the *S* stereochemistry at C11 for both covalent adducts.

Tomaymycin aromatic ring NOE connectivities to DNA, including H9 to 5AH1′, 5AH2, and 6TH1′ (Table 2), demonstrate a head-to-head orientation of the two tomaymycin molecules in the bis-adduct. The orientation of the aromatic rings in the DSB-120 is fixed in the same head-to-head orientation by the methylene linker unit.

Comparison of the Structures of the Bis-tomaymycin and DSB-120 10-mer Duplex Adducts. The majority of the nonexchangeable proton resonances are well resolved in the two-dimensional NMR experiments for both the bis-tomaymycin and DSB-120 10-mer adducts in D_2O buffer. Proton resonance assignments, with the exception of H5′ and H5″ protons, due to spectral overlap, were completed by established methods using two-dimensional through-space (NOESY) and through-bond (DQF-COSY) couplings.[18]

A. Two-Dimensional NOESY and COSY Experiments. Panel B of Figure 7 shows an expanded NOESY contour plot of the regions establishing connectivities between the base protons and the deoxyribose H1′ protons for the DSB-120 10-mer duplex cross-linked adduct. Each purine H8 and pyrimidine H6 proton exhibits NOEs to its own H1′ proton and the H1′ of the sugar of the 5′ flanking nucleotide, characteristic of a right-handed duplex. This permits the chain to be traced from 1C to 10G in the DSB-120 self-complementary 10-mer duplex adduct (panel B). Only the expanded region showing 8I NOE connectivities is displayed for the bis-tomaymycin adduct (panel A). The 8I site exhibits distinct behavior in the DSB-120 adduct, with an unusually weak connectivity from 8IH1′ to 7CH6 compared to that for the bis-tomaymycin adduct (arrowheads in panels A and B, Figure 7).

The expanded DQF-COSY plot showing through-bond *J*-couplings for H1′−H2″ and H1′−H2′ for the DSB-120 decamer adduct demonstrates an unusual feature for the 8I nucleotide of the DSB-120 duplex adduct (unpublished results). Typically, the chemical shifts of H2′ protons are upfield of H2″ within the same nucleotide of a DNA sequence.[18] However, for the 8I nucleotide

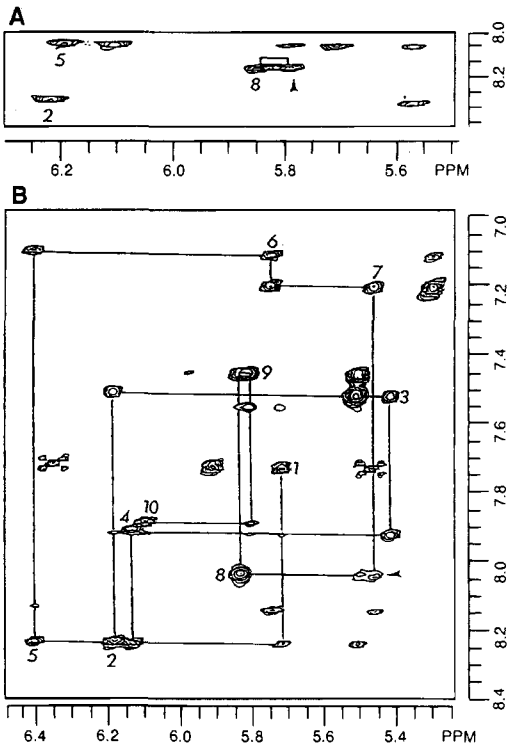

Figure 7. Two-dimensional phase-sensitive NOESY (250-ms mixing time) expanded contour plots of the (A) bis-tomaymycin d(CICGATCICG)$_2$ and (B) DSB-120 d(CICGATCICG)$_2$ adducts in D_2O-buffered solution, pH 6.8, 100 mM sodium chloride, and 10 mM sodium phosphate at 23 °C, demonstrating NOE connectivities for each PuH8/PyH6 to its own deoxyribose H1′ protons (denoted with nucleotide number corresponding to position in the sequence) and to the H1′ proton of its 5′ neighbor. Arrowhead denotes 8I(H8) to 7C(H1′) internucleotide through-space NOESY connectivity.

in the DSB-120 adduct, this pattern is reversed (Table 1), and in addition, the intense coupling for H1′−H2′ is downfield of the weaker H1′−H2″ coupling for the 8I nucleotide (unpublished results). This is found exclusively in the DSB-120 decamer adduct. The reversal of chemical shift for these protons is usually associated with terminal nucleotides or with internal nucleotides that have undergone a conformational change. The magnitude of this effect is less in the bis-tomaymycin decamer adduct, where the H2′ and H2″ resonances

overlap (Table 1). However, the evidence is consonant with other spectral features unique to the DSB-120 adduct that have been previously identified and augments the evidence that DSB-120 does induce an additional perturbation in structure of the nucleotide facing the covalently modified guanine in the minor groove. This deviation is not found in the bis-tomaymycin adduct.

B. Nucleic Acid Proton Chemical Shifts. Chemical shifts for oligonucleotide proton resonance signals are listed in Table 1. There are upfield chemical shifts of 0.28 and 0.30 ppm for 7CH6 and 0.24 and 0.28 ppm for 7CH5 relative to the duplex for the bis-tomaymycin and DSB-120 10-mer adducts, respectively. Furthermore, there are 0.30 and 0.21 ppm downfield shifts for 3CH6 and 3CH5, respectively, that are uniquely observed for the DSB-120 adduct relative to the duplex. These chemical shift changes suggest that there is a modest increase in stacking of the 6T–7C step for both adducts but destacking of the 2I–3C step only occurs in the DSB-120 adduct. The 8IH2 resonance shows a 0.40 ppm upfield shift relative to the duplex but only for the bis-tomaymycin adduct. This can be rationalized due to the location of 8IH2 within the shielding zone of the tomaymycin ethylidene functionality, which is absent in the DSB-120 structure. The 0.40 ppm downfield shift relative to the duplex of the 5AH2 proton resonance signal found for both DNA adducts can be attributed to the proximity of this proton to the deshielding zone of the aromatic ring of the covalently attached drug. The chemical shifts of the imino protons for each adduct are similar, which argues against differences in base-pair hydrogen bonding (Table 1).

For both drug–DNA adducts, changes in chemical shifts of deoxyribose protons such as 4GH1′ are of a similar magnitude and mostly restricted to the minor groove in proximity to the drug overlap region with DNA. Upon examination of the models, most of these shifts are attributable to drug shielding or deshielding effects. The most dramatic difference between adducts occurs for 6TH4′. While this proton is shielded by the drug aromatic rings in both adducts, the upfield shift relative to the free duplex is attenuated in the DSB-120 adduct (1.65 ppm) relative to the bis-tomaymycin adduct (2.28 ppm). This observation suggests that the tomaymycin aromatic ring more directly faces the wall of the minor groove, where 6TH4′ would receive the full force of shielding, while the structure assumed in interstrand DNA cross-linking via tethered DNA-reactive units causes the DSB-120 aromatic ring to be partially averted from the wall of the groove and directed toward the floor.

C. Intermolecular Drug–DNA Contacts. The proton resonances for DSB-120 and tomaymycin in the 10-mer adducts have been assigned through analysis of the NOESY and correlated COSY spectra recorded in D_2O at 23 °C. NOESY cross-peaks are observed that permit establishment of intermolecular proton–proton contacts (<5 Å) between DSB-120 or tomaymycin and 4G, 5A, 6T, 7C, and 8I residues (Table 2).

For both adducts, a complete network of cross-peaks firmly locates the drugs within the minor groove of the duplex. In both cases, H11 shows a strong cross-peak connectivity to 5AH1′ and a moderate to weak cross-peak connectivity to 4GH1′ (cross-peaks A and B, respectively, in Figure 6). The weak cross-peak connectivity of H11 to 5AH4′ in the bis-tomaymycin adduct contrasts with the moderate cross-peak connectivity of H11 to the same proton in the DSB-120 adduct (cross-peak C in Figure 6). As previously established (see before), the difference in the degree of upfield chemical shift of the tomaymycin and DSB-120 6TH4′ resonance signals suggests that the tomaymycin aromatic ring adopts a more face-on orientation to the wall of the groove compared to that in DSB-120. This conclusion is supported by the fact that a more edge-on stance for the inner edge of DSB-120 would swing the H11 proton into closer proximity to the 5AH4′ proton, resulting in a more intense NOE.

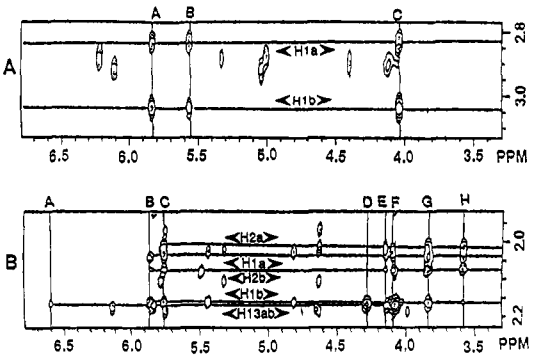

Figure 8. Expanded contour plot of the two-dimensional phase-sensitive NOESY spectrum (250-ms mixing time) of the (A) bis-tomaymycin d(CICGATCICG)$_2$ and (B) DSB-120 d(CICGATCICG)$_2$ adducts in 0.5 mL of D_2O-buffered solution, pH 6.8, 100 mM sodium chloride, and 10 mM sodium phosphate at 23 °C, establishing through-space connectivities from P[1,4]B pyrrolo and H13 protons to DNA protons. (A) Tomaymycin H1a and H1b through-space connectivities to A, 8I(H1′); B, tomaymycin(H11); C, tomaymycin(H11a). (B) DSB-120 through-space connectivities are A, DSB-120(H13)–DSB-120(H9); B, DSB-120(H1a, H1b)–8I(H1′); C, DSB-120(H1a, H1b, H2a, H2b)–DSB-120(H11); D, DSB-120(H13)–DSB-120(H12); E, DSB-120(H1a, H1b, H2a, H2b)–5A(H4′); F, DSB-120(H1a, H1b, H2a, H2b)–9C(H4′) and DSB-120(H13)–7C(H4′); G, DSB-120(H1a, H1b, H2a, H2b)–DSB-120(H3b) and DSB-120(H13)–DSB-120(7OCH$_3$); H, DSB-120(H1a, H1b, H2a, H2b)–DSB-120(H3a).

The methylene protons of the linker of DSB-120 (H12a, H12b, H13a, and H13b) exhibit NOESY connectivities that locate them in the minor groove (Table 2). Characteristic of this location are the overlapping resonance signals H13a and H13b, which each display a strong cross-peak connectivity to 7CH4′ (cross-peak F in Figure 8B). The overlapping resonances H12a and H12b are similarly located in proximity to 5AH2 and 6TH1′ (Table 2).

Additional observed NOESY cross-peaks demonstrate that the DSB-120 interstrand cross-linker adopts a conformation in other regions distinct from that of the bis-tomaymycin adducts in the 10-mer duplex. The ethylidene methyl protons (H13) of tomaymycin show cross-peak connectivities to resonances 8IH2, 8IH1′, 9CH1′, and 9CH4′ on the floor and wall of the minor groove (Table 2). For DSB-120 and tomaymycin, H1a and H1b serve as probes for the depth of minor groove penetration. For tomaymycin, H1a and H1b, which are located along the inner edge of the drug, exhibit cross-peak connectivities to 8IH1′ (cross-peak A in Figure 8A) and 8IH2 (Table 2). The 8IH1′ and 8IH2 protons are positioned on the wall and the floor of the minor groove, respectively. In the case of DSB-120, NOESY cross-

peak intensities indicate a shallower immersion of the five-membered ring because DSB-120 H1a and H1b show reduced through-space NOE cross-peak connectivities to 8IH1′ (cross-peak B in Figure 8B) and 8IH2 (Table 2). At the same time, weak DSB-120 H1a and H1b cross-peak connectivities to 5AH4′ and 7CH4′, which are located on the periphery of the minor groove, are now observed (cross-peaks E and F, respectively, in Figure 8B). These cross-peak connectivities are not observed in the tomaymycin adduct. From these sets of data, it appears that the ends of the DSB-120 molecule bow up away from the floor of the groove in the interstrand cross-linked DNA adduct. Previous energy-minimization calculations on the DSB-120 10-mer adduct had indicated that a three-methylene linker unit would be shorter than the optimum distance needed to comfortably accommodate cross-linking the guanines four base pairs apart in this sequence without distortion.[16b] The bowing up of the pyrrolo rings of DSB-120 in the covalent adduct may be the structural response to this strain.

Discussion

A comparison of the two-dimensional NMR spectra of the bis-tomaymycin and DSB-120 10-mer adducts offers some insight into the usefulness of structural characterization of DNA bis-adducts as a guide to DNA cross-linker design. The synthesis of dimeric analogs that cross-link DNA has been readily accomplished.[12] The consequences are that such potent agents can, depending on the case, induce novel DNA distortion,[13] exhibit an altered sequence selectivity,[14] and possess different stabilities on DNA relative to the monoalkylating parent.[12b,15] The study described here permits assessment of the achievements and limitations of a strategy of template-directed cross-linker design[16] based on a monoalkylating unit such as tomaymycin that induces only slight distortion of DNA.

A summary of the major findings of this study are (1) that both drugs form self-complementary adducts with the d(ClCGATClCG)$_2$ duplex sequence. (2) The covalent linkage sites occur between C11 of either drug and the exocyclic 2-amino group of the single reactive guanine on each strand of d(ClCGATClCG)$_2$. In the case of DSB-120, this is evidence for the formation of a guanine–guanine DNA interstrand cross-link. (3) The formation of an ***S*** stereochemistry at the covalent linkage site with an associated 3′ orientation. (4) While the majority of DNA in these adducts appears to be B-form, DSB-120 interstrand cross-linking induces atypical properties in the 8I nucleotide, indicated by broadening of the 8IH2 proton resonance, non-C2′endo sugar geometry (from COSY coupling patterns), and unusually weak internucleotide NOE connectivity to the 7C nucleotide. Tomaymycin does not produce this regional dislocation. (5) For tomaymycin, while there are strong NOE connectivities from protons on the five-membered ring to the 8IH2 proton on the floor of the minor groove, the equivalent internucleotide connectivities in DSB-120 are weaker. This indicates that the tomaymycin tail is close to the floor of the minor groove, while the five-membered ring of DSB-120 is more shallowly immersed, perhaps due to strain from cross-linking with a very short linker unit. (6) The conformational stresses induced on the duplex by DSB-120 appear to make the region of covalent attachment more accessible to solvent

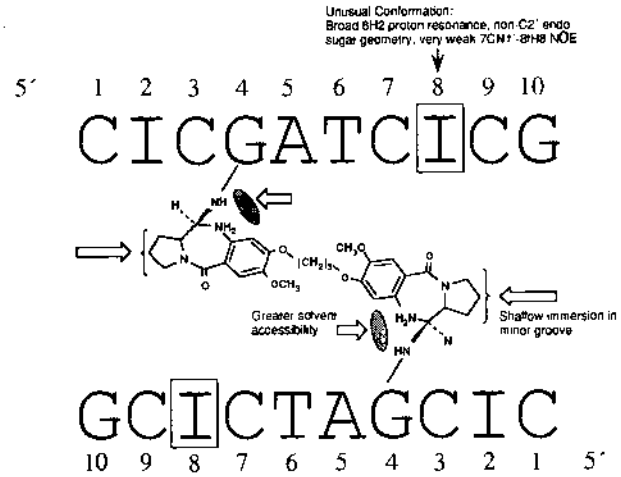

Figure 9. Summary of unusual properties of the DSB-120 5′CGA′^{10} cross-linked adduct.

than is the case for tomaymycin. The 4GN2H$_b$ resonance appears in 100% D_2O on the tomaymycin adduct but is only observed in 90% H_2O/10% D_2O for the DSB-120 adduct. The unusual properties of the DSB-120 10-mer duplex adduct are summarized in Figure 9.

Analysis of Slightly Distorted Bis-drug-Modified Self-Complementary Duplex Templates Is Predictive of the Site of Covalent Linkage and the Orientation and Stereochemistry for Analogous Dimeric DNA Cross-Linkers. One important goal in medicinal chemistry is to synthesize molecules that will react with their molecular target in a defined and predictable way. In the case of DNA-reactive drugs, such as the P[1,4]Bs, that bond within the minor groove, identifying the options first entails defining the nucleotide and sequence selectivity, the groove orientation, and the stereochemistry at the covalent linkage site.

For example, following establishment of the P[1,4]B sequence selectivity by footprinting methods,[6] work from this laboratory documented the sequence-dependency of both stereochemistry and drug orientation in the minor groove.[2c,16,17] Bonding sequences such as (ATGC-AT)$_2$ (P[1,4]B-bonding triplet underlined) yielded a mixture of tomaymycin 3′*S* and 5′*R* adducts.[2d] Single 3′*S* self-complementary bis-tomaymycin adducts were formed with the d(ClCGAATTClCG)$_2$ and d(ClCGA-TClCG)$_2$ sequences.[16] In the latter case, two tomaymycin molecules on opposite strands were separated by a distance suitable for inserting a short linker between head-to-head aromatic rings. All attempts to design a sequence-unique tail-to-tail orientation of a bis-tomaymycin adduct resulted in a complex mixture of adducts.[16b] Molecular modeling of the d(ClCGATClCG)$_2$ sequence led to the proposal for (-CH2-)$_n$-linked tomaymycin DNA interstrand cross-linkers.[18b] Linkage through an ether at C8 was chosen since the C8 methoxy unit of tomaymycin is directed along the floor of the minor groove and C7-linked P[1,4]B dimeric analogs have been shown to be easily reversible from linear plasmid DNA.[12b]

With only this knowledge, a strategy of template-directed drug design would logically (1) select sequence B (Figure 3) as the template, for which the bis-adduct is well defined, (2) favor synthesis of a compound linked in a head-to-head fashion at the aromatic rings, for which the orientation of a single bis-adduct can be defined, (3) enact the linkage through C8 of the aromatic

ring, and (4) predict the formation of *S* stereochemistry at the covalent linkage site. In fact, DSB-120 does form a single adduct cross-linked on sequence B with covalent modification at 4G. This cross-linked adduct has *S* stereochemistry at C11, as in the bis-adduct. Both the bis-tomaymycin and DSB-120 adducts maintain self-complementarity as well. Since the DSB-120 adduct with other sequences has not been structurally characterized and tail-to-tail P[1,4]B−DNA cross-linkers have not been synthesized, it is difficult to determine how the behavior of such adducts would relate to the bis-adduct models. Nevertheless, when a uniquely defined, relatively nondistortive bis-adduct is chosen as a template for an analogy-based cross-linker, the evidence here suggests that there is a high likelihood that it will cross-link DNA at a predictable location and that essential features of the covalent modification can be preserved.

Analysis of Bis-adduct Templates Does Not Predict the Precise Nature of DNA Structural Accommodation to Interstrand Cross-Linking. The P[1,4]-Bs induce minimal bending in DNA.[19] However, they are considered to be relatively nondistortive compared to monoalkylating drugs like *cis*-platinum, psoralen, and the CPIs derived from (+)-CC-1065. The bis-adduct template-directed approach to drug design of an *interstrand* DNA cross-linker was less successful for the CPIs, which alkylate N3 of adenine. In that case, a sequence designed to form an *interstrand* bis-adduct was instead found to form an *intrastrand* bis-adduct.[20] We believe this is due to the first CPI monalkylation inducing significant distortion in the DNA, which alters the reactivity of the remaining adenines.

For the bis-tomaymycin 10-mer adduct, the formation of a template interstrand bis-adduct with little distortion of DNA was achieved. Nonetheless, there are features of the DSB-120 interstrand cross-link that indicate changes in both DNA and DSB-120, imposed exclusively by the cross-linking that is not anticipated by the bis-adduct template. In the case of the DSB-120 10-mer adduct, two-dimensional NMR evidence indicates induced conformational changes in the 8I nucleotide, the adoption by the antibiotic aromatic ring of a more face-on disposition to the floor of the minor groove, and a bowing up of the edges of the drug away from the floor of the minor groove. In the case of DSB-120, this last effect may be due to the methylene bridge being too short to comfortably accommodate cross-linking. The combination of these distortions appears to enhance solvent accessibility to the vicinity of covalent modification, indicated by the enhanced exchange of the 4GN2H_b proton in the DSB-120 adduct relative to the bis-tomaymycin adduct.

Several homologs of DSB-120 have been synthesized that could test the basis for this distortion and, ultimately, its contribution to the biological properties of this drug.[15] Dimeric analogs containing three to six methylene units in the linker have been made. There is a significant correlation between DNA-binding affinity, cross-linking efficiency, and cytotoxicity.[15] Homologs with an odd number of methylenes (three or five) display significant effects, while those with an even number do not. Solution structures of these analogs could be of use in determining the structural basis for optimization of the linker distance and its contribution to conformational dislocation of cross-linked DNA.

Experimental Procedures

Chemicals. Tomaymycin 11-methyl ether was obtained from Fujisawa Pharmaceuticals. DSB-120 was synthesized as described previously.[1] Reagents used to prepare the NMR buffer, sodium phosphate (99.99%) and sodium chloride (99.9%), were purchased from Aldrich. HPLC-grade water and methanol were purchased from Baxter Scientific and Fisher, respectively.

Oligonucleotide Preparation and Purification. d-(CICGATCICG)$_2$ was made on an Applied Biosystems 381A instrument and purified across a Machery-Nagel Nucleogen-DEAE 60-7 HPLC column with an increasing gradient to 1 M NaCl in 15 mM sodium phosphate and 20% acetonitrile/aqueous buffer, pH 6.8.

Adduct Preparation and Purification. The tomaymycin and DSB-120 adducts were prepared by adding drug (~4 mg in 0.2 mL of HPLC-grade methanol) to buffered solutions of the purified 10-mer duplex (25 mg in 0.6 mL of 20 mM sodium phosphate, 200 mM NaCl, pH 6.85) and stirring the reaction mixture at room temperature for 5 days. Duplex adduct was separated from excess drug by fractionation on a hydroxyapatite column with a slower linear gradient of aqueous sodium phosphate buffer, pH 6.8, increasing from 10 to 200 mM, monitoring UV absorbance at 254 nm. The adduct fraction was desalted across Water Associates C18 Sep-pak cartridges, lyophilized, dissolved in 0.5 mL of aqueous buffer (10 mM sodium phosphate, 100 mM NaCl, pH 6.85), and relyophilized for storage at −20 °C.

NMR Experiments. One- and two-dimensional 500-MHz ^{1}H- and 202.44-MHz ^{31}P-NMR data sets were recorded at 23 °C on a General Electric GN-500 NMR spectrometer. Chemical shifts are reported (ppm) with positive values downfield from an external reference of 1 mg/mL TSP in D_2O for ^{1}H resonances (HOD resonance was set to 4.751 ppm) and an external reference of 85% H_3PO_4 in D_2O for ^{31}P resonances. Approximately 25−28 mg of the buffered duplex or duplex adducts in 0.5 mL of 99.96% D_2O was prepared.

For all two-dimensional experiments, a presaturation pulse was applied to suppress the HOD signal. Two-dimensional heteronuclear phosphorus-detected ^{31}P−^{1}H phase-sensitive COSY experiments for the duplex adducts were performed according to published procedures.[21] Homonuclear scalar coupling was determined using the standard phase-sensitive two-dimensional double-quantum-filtered COSY.[22] Sixty-four scans were collected with a 1.0-s pulse repetition time for each of the 256 FIDs in the t_1 dimension to generate 2 × 256 × 2048 data matrices. Data for the phase-sensitive two-dimensional NOESY spectra were collected at a 250-ms mixing time using the States hypercomplex method.[23] Thirty-two scans with a 2-s pulse repetition time were collected for each of the 512 FIDs in the t_1 dimension to generate 2 × 512 × 2048 data matrices. For all proton two-dimensional phase-sensitive experiments, a 45° shifted sine bell function was applied to the data in both dimensions prior to transformation. Data sets were zero-filled twice in the t_1 dimension such that the final frequency domain spectra consisted of 1K × 1K data matrices.

Acknowledgment. This research was supported by grants from the Public Health Service (CA-49751), the Welch Foundation, The Upjohn Co., and the Burroughs Wellcome Scholars Program. Funding for John Mountzouris was from the American Foundation for Pharmaceutical Education and the Warner Lambert Predoctoral Fellowship from the Division of Medicinal Chemistry of ACS. We are grateful to David Bishop for editorial assistance and preparation of the manuscript.

Supplementary Material Available: Two figures (3 pages). Ordering information is given on any current masthead page.

References

(1) Bose, D. S.; Thompson, A. S.; Ching, J.; Hartley, J. A.; Berardini, M. J.; Jenkins, T. C.; Neidle, S.; Hurley, L. H.; Thurston, D. E. Rational Design of a Highly Efficient Irreversible DNA Interstrand Cross-Linking Agent Based on the Pyrrolobenzodiazepine Ring System. *J. Am. Chem. Soc.* **1992**, *114*, 4939–4941.

(2) (a) Hurley, L. H.; Petrusek, R. L. Proposed Structure of the Anthramycin–DNA Adduct. *Nature* **1979**, *282*, 529–531. (b) Graves, D. E.; Pattaroni, C.; Krishnan, B. S.; Ostrander, J. M.; Hurley, L. H.; Krugh, T. R. The Reaction of Anthramycin with DNA. Proton and Carbon Nuclear Magnetic Resonance Studies on the Structure of the Anthramycin–DNA Adduct. *J. Biol. Chem.* **1984**, *259*, 8202–8209. (c) Barkley, M. D.; Cheatham, S.; Thurston, D. E.; Hurley, L. H. Pyrrolo(1,4)benzodiazepine Antitumor Antibiotics. Evidence for Two Forms of Tomaymycin Bound to DNA. *Biochemistry* **1986**, *25*, 3021–3031. (d) Cheatham, S.; Kook, A.; Hurley, L. H.; Barkley, M. D.; Remers, W. One- and Two-Dimensional ^{1}H NMR, Fluorescence and Molecular Modeling Studies on the Tomaymycin–d(ATGCAT)2 Adduct. Evidence for Two Covalent Adducts with Opposite Orientations and Stereochemistry at the Covalent Linkage Site. *J. Med. Chem.* **1988**, *31*, 583–590.

(3) Mountzouris, J. A.; Hurley, L. H. Unpublished results.

(4) Kohn, K. W. Anthramycin. In *Antibiotics III. Mechanism of Action of Antimicrobial and Antitumor* Agents; Corcoran, J. W., Hahn, F. E., Eds.; Springer-Verlag: New York, 1975; pp 3–11.

(5) Petrusek, R. L.; Uhlenhopp, E. L.; Duteau, N.; Hurley, L. H. Reaction of Anthramycin with DNA. Biological Consequences of DNA Damage in Normal and Xeroderma Pigmentosum Cell Lines. *J. Biol. Chem.* **1982**, *257*, 6207–6216.

(6) Hertzberg, R. P.; Hecht, S. M.; Reynolds, V. L.; Molineux, I. J.; Hurley, L. H. DNA Sequence Specificity of the Pyrrolo[1,4]-benzodiazepine Antitumor Antibiotics. Methidiumpropyl-EDTA-Iron(II) Footprinting Analysis of DNA Binding Sites for Anthramycin and Related Drugs. *Biochemistry* **1986**, *25*, 1249–1258.

(7) Hurley, L. H.; Reck, T.; Thurston, D. E.; Langley, D. R. Pyrrolo-[1,4]benzodiazepine Antitumor Antibiotics: Relationship of DNA Alkylation and Sequence Specificity to the Biological Activity of Natural and Synthetic Compounds. *Chem. Res. Toxicol.* **1988**, *1*, 258–268.

(8) Pierce, J. R.; Nazimiec, M.; Tang, M.-S. Comparison of Sequence Preference of Tomaymycin- and Anthramycin-DNA Bonding by Exonuclease III and l Exonuclease Digestion and UvrABC Nuclease Incision Analysis. *Biochemistry* **1993**, *32*, 7069–7078.

(9) Cargill, C.; Bachmann, E.; Zbinden, G. Effects of Daunomycin and Anthramycin on Electrocardiogram and Mitochondrial Metabolism of the Rat Heart. *J. Natl. Cancer Inst.* **1974**, *53*, 481–486.

(10) (a) Pratt, W. B.; Ruddon, R. W. *The Anticancer Drugs*; Oxford University Press: New York, 1979. (b) Gale, E. F.; Cundliffe, E.; Reynolds, P. E.; Richmond, M. H.; Waring, M. J. *The Molecular Mechanism of Antibiotic Action*, 3rd ed.; Wiley: New York, 1981. (c) Armstrong, R. W.; Salvati, M. E.; Nguyen, M. Novel Interstrand Cross-Links Induced by the Antitumor Antibiotic Carzinophilin/Azinomycin B. *J. Am. Chem. Soc.* **1992**, *114*, 3144–3145.

(11) (a) Kohn, K. W. DNA Damage in Mammalian Cells. *Bioscience* **1981**, *31*, 593–597. (b) Kohn, K. W. DNA Crosslinking Agents. In *Development of Target-Oriented Anticancer Drugs*; Chen, Y.-C., Goz, B., Minkoff, M., Eds.; Raven Press: New York, 1983; pp 181–188.

(12) (a) Mitchell, M. A.; Kelly, R. C.; Wicnienski, N. A.; Hatzenbuhler, N. T.; Williams, M. G.; Petzold, G. L.; Slightom, J. L.; Siemieniak, D. R. Synthesis and DNA Cross-Linking by a Rigid CPI Dimer. *J. Am. Chem. Soc.* **1991**, *113*, 8994–8995. (b) Farmer, J. D.; Rudnicki, S. M.; Suggs, J. W. Synthesis and DNA Crosslinking Ability of a Dimeric Anthramycin Analog. *Tetrahedron Lett.* **1988**, *29*, 5105–5108. (c) Qu, Y.; Farrell, N. Interaction of Bis(platinum) Complexes with the Mononucleotide 5′-Guanosine Monophosphate. Effect of Diamine Linker and the Nature of the Bis(platinum) Complex on Product Formation. *J. Am. Chem. Soc.* **1991**, *113*, 4851–4857.

(13) Seaman, F. C.; Hurley, L. H. Interstrand Cross-Linking by Bizelesin Produces a Watson-Crick to Hoogsteen Base-Pairing Transition Region in d(CGTAATTACG)$_2$. *Biochemistry* **1993**, *32*, 12577–12585.

(14) Sun, D.; Hurley, L. H. Analysis of the Monoalkylation and Cross-Linking Sequence Specificity of Bizelesin, a Bifunctional Alkylation Agent Related to (+)-CC-1065. *J. Am. Chem. Soc.* **1993**, *115*, 5925–5933.

(15) Bose, D. S.; Thompson, A. S.; Smellie, M.; Barardini, M. D.; Hartley, J. A.; Jenkins, T. C.; Neidle, S.; Thurston, D. E. Effect of Linker Length on DNA-binding Affinity, Cross-Linking Efficiency and Cytotoxicity of C8-Linked Pyrrolobenzodiazepine Dimers. *J. Chem. Soc., Chem. Commun.* **1992**, *20*, 1518–1520.

(16) (a) Boyd, F. L.; Cheatham, S. F.; Remers, W.; Barkley, M. D.; Hurley, L. H. Characterization of the Tomaymycin–d(CICGAATTCICG)$_2$ Adduct Containing Two Drug Molecules per Duplex by NMR, Fluorescence, and Molecular Modeling Studies. *Biochemistry* **1990**, *29*, 2387–2403. (b) Wang, J.-J.; Hill, G. C.; Hurley, L. H. Template-Directed Design of a DNA–DNA Cross-Linker Based upon a Bis-Tomaymycin-Duplex Adduct. *J. Med. Chem.* **1992**, *35*, 2995–3002.

(17) Boyd, F. L.; Cheatham, S. F.; Remers, W.; Hill, G. C.; Hurley, L. H. Characterization of Structure of the Anthramycin–d(ATGCAT)$_2$ Adduct by NMR and Molecular Modeling Studies. Determination of the Stereochemistry at the Covalent Linkage Site, Orientation in the Minor Groove, and Effect of Drug Binding on Local DNA Structure. *J. Am. Chem. Soc.* **1990**, *112*, 3279–3289.

(18) Reid, B. R. Sequence-specific Assignments and Their Use in NMR Studies of DNA Structure. *Q. Rev. Biophys.* **1987**, *20*, 1–33.

(19) Kizu, R.; Draves, P. H.; Hurley, L. H. Correlation of DNA Sequence Specificity of Anthramycin and Tomaymycin with Reaction Kinetics and Bending of DNA. *Biochemistry* **1993**, *32*, 8712–8722.

(20) Seaman, F. C.; Hurley, L. H. Unpublished results.

(21) Bax, A.; Sarkar, S. Elimination of Refocusing Proton Pulses in NMR Experiments. *J. Magn. Reson.* **1984**, *60*, 170–176.

(22) Shaka, A. J.; Freeman, R. J. Simplification of NMR Spectra by Filtration through Multiple-Quantum Coherence. *J. Magn. Reson.* **1983**, *51*, 169–173.

(23) States, D. J.; Haberkorn, R. A.; Ruben, D. J. A Two-Dimensional Nuclear Overhauser Experiment with Pure Absorption Phase in Four Quadrants. *J. Magn. Reson.* **1982**, *48*, 286–292.